Available online at www.sciencedirect.com
SCIENCE DIRECT®
Journal of Magnetic Resonance 165 (2003) 175–179
JMR Journal of Magnetic Resonance
www.elsevier.com/locate/jmr

Communication

Low field intermolecular double-quantum coherence imaging via the Overhauser effect

Wilson Barros Jr.,[a,*] Paulo Loureiro de Sousa,[b] and M. Engelsberg[a]

[a] Departamento de Física, Universidade Federal de Pernambuco, 50670-901 Recife, Pernambuco, Brazil
[b] Institut de Physique Biologique, Université Louis Pasteur, UMR 7004-CNRS, 4, rue Kirschléger, 67085 Strasbourg Cedex, France

Received 6 May 2003; revised 29 July 2003

Abstract

Intermolecular double-quantum coherence (i-DQC) signals in liquids are usually associated with high magnetic fields. We demonstrate that, in a magnetic field of only 16 mT, i-DQC imaging of water protons is feasible thanks to the nuclear magnetization enhancement produced by the Overhauser effect. i-DQC images of a phantom containing an aqueous solution of a trityl free radical, with phase encoding in the DQC evolution period or in the acquisition period, are presented. Possible applications of low field i-MQC images are proposed.

Keywords: MRI; i-MQC; Low field; Overhauser; CRAZED

1. Introduction

Since the roles of the dipolar coupling between distant spins in liquids and the classical demagnetizing field became clearly understood, a wealth of possible applications exploiting these effects has emerged [1–8]. Although some debate over quantum mechanical versus classical interpretations persisted for some time, it now appears that both approaches yield identical results in most experiments [9–11]. It is therefore customary to also refer to these effects as intermolecular multiple-quantum coherences (i-MQC) [12].

The CRAZED (COSY revamped with asymmetric z-gradient echo detection) experiment [12], and its variations, proved to be of central importance in the clarification of i-MQC effects as well as in many of their practical applications. Under the action of the classical demagnetizing field, the net effect can be described as if an n quantum evolution takes place in the time interval t_1 between the first $(\pi/2)_y$ RF pulse and the second $\beta = \pi/2$ pulse. In this i-MQC evolution interval, a magnetic field gradient pulse of area GT is applied. A second gradient pulse of area nGT is further applied in the acquisition period after the β pulse. This second gradient converts the multiple-quantum coherence into single-quantum coherence as predicted by a quantum mechanical treatment [13]. For an isochromat with offset angular frequency $\Delta\omega$ in the rotating frame, the transverse magnetization $M_+ = M_x + iM_y$ can be shown [14] to evolve according to $\exp(-in\Delta\omega t_1)\exp(i\Delta\omega t_2)$, where t_2 denotes time measured from the β pulse. The magnetic field gradient is applied along the z-direction and an initially uniform distribution of magnetization, produced by a polarizing field $B_0\hat{z}$, is assumed.

Since the distribution of isochromats caused, for example, by a slightly imperfect polarizing field, refocuses at $t_2 = nt_1$, an echo signal unambiguously attributable to long-range dipolar couplings is observable.

Lee et al. [14] derived an expression for the i-MQC signal amplitude that can be readily generalized to include transverse relaxation time T_2. For $n = 2$, $\Delta\omega = 0$, and $\beta = \pi/2$ the result is:

$$M_+(t_1,t_2) = iM_0(2\tau_d/t_2)J_2\left[\frac{-t_2\exp(-t_1/T_2)}{\tau_d}\right]\exp(-t_2/T_2). \quad (1)$$

* Corresponding author. Fax: +558132718450.
E-mail addresses: wilson@df.ufpe.br (W. Barros Jr.), mario@df.ufpe.br (M. Engelsberg).

1090-7807/$ - see front matter © 2003 Elsevier Inc. All rights reserved.
doi:10.1016/S1090-7807(03)00277-5

The above signal amplitude, corresponding to the original CRAZED sequence, can actually be increased by a factor $3\sqrt{3}/4$ by choosing $\beta = 2\pi/3$ [15].

The demagnetizing time $\tau_d = 1/\gamma\mu_0 M_0$ plays a central role in the signal amplitude given by Eq. (1). Here, M_0 denotes the thermal equilibrium magnetization, γ is the magnetogyric ratio, and μ_0 is the vacuum permeability. Neglecting relaxation, the i-DQC signal amplitude has its first maximum for $t_2/\tau_d = 2.15$. This is somewhat lower than the value where the second order Bessel function J_2 in Eq. (1) reaches its first maximum. Moreover, if $t_2 \ll \tau_d$, T_2, as will be chosen to be the case in our images, the expansion of J_2 for small arguments leads to a linear regime $M_+ \approx (iM_0/4)(t_2/\tau_d)$. If, on the other hand, relaxation effects become important, the maximum is shifted to lower values of t_2/τ_d. This would suggest that larger values of τ_d could become tolerable, for a given value of t_2, if one wants to reach the signal maximum. However, in this situation, the loss of signal caused by transverse relaxation becomes the dominant effect and the signal amplitude at the maximum is substantially degraded. Thus, in either case, τ_d must be kept as short as possible and, consequently, M_0 as large as possible to avoid a sizable decay.

For pure water at a magnetic field $B_0 = 14.08\,\mathrm{T}$, the demagnetizing time has a value of only $\tau_d = 67\,\mathrm{ms}$ [16]. Therefore, transverse relaxation effects should be almost negligible at the signal maximum for such a high magnetic field. This maximum theoretical signal can be estimated from Eq. (1) to be 36% of the equilibrium magnetization signal amplitude [17]. However, values obtained in practice have been more frequently found to be in the range 10–15% mainly due to the effects of diffusion and radiation damping [14,17,18].

Although the above results appear to predict that the study of i-DQC effects in liquids would be restricted in practice to high magnetic fields, it will be demonstrated in this communication that this need not be the case. Indeed at a magnetic field as low as 16 mT, not only are i-DQC signals, but also i-DQC imaging will be shown to be feasible. Given the extremely long value $\tau_d = 59\,\mathrm{s}$ of the demagnetizing time of water at $B_0 = 16\,\mathrm{mT}$, the i-DQC signal amplitude predicted by Eq. (1) can be expected to be only an exceedingly small fraction of an initially quite small signal. However, the enhancement of the nuclear magnetization, brought about by the electronic Overhauser effect involving a dissolved free radical, can rescue the i-DQC effect even at such low fields.

The theoretically expected Overhauser enhancement of the proton resonance in water depends upon several factors [19] such as free radical concentration, the type of radical, and the amplitude and duration of the RF field at the EPR frequency.

i-MQC effects at very low magnetic field offer some interesting possibilities. The combination of the peculiar contrast attainable by i-DQC imaging when half the pitch π/γGT of the magnetization helix is tuned to the dimensions of a liquid structure [20], and the lack of any appreciable bulk magnetization artifact [21] afforded by a very low magnetic field, could prove to be valuable. Furthermore, the large sensitivity to small changes of water mobility, inherent to the Overhauser enhancement, and its effect upon i-DQC could also be useful for some applications. If water molecules become less mobile, for example by chemical exchange or other processes, the enhancement can be strongly suppressed. This property has been shown to be quite valuable to probe the spatio-temporal evolution of various transport processes [22,23].

Experiments were performed in a home-built imaging system and magnet [24]. A phantom consisting of an external glass tube, 25 mm in diameter, was filled with an aqueous solution of trityl radical [25]. Two concentric glass tubes, 10 and 4 mm in external diameter, were placed approximately concentrically with the external tube. The wall thickness of each tube was 1 mm and the length of all cylindrical tubes was 20 mm. A solenoidal coil with its axis perpendicular to the $B_0 = 16\,\mathrm{mT}$ polarizing field was employed as a transmit/receive coil for the NMR signal at $\nu_{NMR} = 680\,\mathrm{kHz}$. The much larger volume of this coil compared to that of the sample permitted a radiation damping time $\tau_r = 1/\gamma Q\mu_0(\eta/2)M_0 \approx \frac{1}{3}\tau_d$, of the same order of τ_d [26]. Here, $Q \approx 200$ denotes the quality factor of the coil and $\eta \approx 0.03$ is the filling factor. Furthermore, RF irradiation of the single EPR line of the trityl radical at $\nu_{EPR} = 445\,\mathrm{MHz}$ was provided by 3 cm in diameter birdcage resonator, which, together with its tuning/matching trimmer and coupling circuits, was placed inside the NMR coil and fed by 10 W RF amplifier.

For this phantom, with the above not ideal experimental conditions and a 5 mM trityl concentration, an enhancement of the NMR signal of approximately 30 was obtainable, bringing the value of the demagnetization time to the vicinity of $\tau_d \approx 1.95\,\mathrm{s}$ with a value $\tau_r \sim 0.65\,\mathrm{s}$ for the radiation damping time. The main question posed by this work is whether, given the signal amplitude predicted by Eq. (1) for the transverse relaxation time prevailing in the 5 mM trityl free radical solution, an i-DQC signal would be observable in spite of the non-idealities. A calculation of the maximum i-DQC signal amplitude for $t_1 = 20$ and $t_2 = 200\,\mathrm{ms}$, based upon a simple extension of Eq. (1) with a value of τ_d simply scaled by the enhancement, would yield 2% of the signal corresponding to the Overhauser-enhanced magnetization, for $T_2 = 1.25\,\mathrm{s}$.

Fig. 1 shows schematically the pulse sequence employed to produce two-dimensional i-DQC low field Overhauser images of the cylindrical phantom whose axis is assumed to be along the y-direction. Referring to the RF channels of Fig. 1, EPR excitation takes place

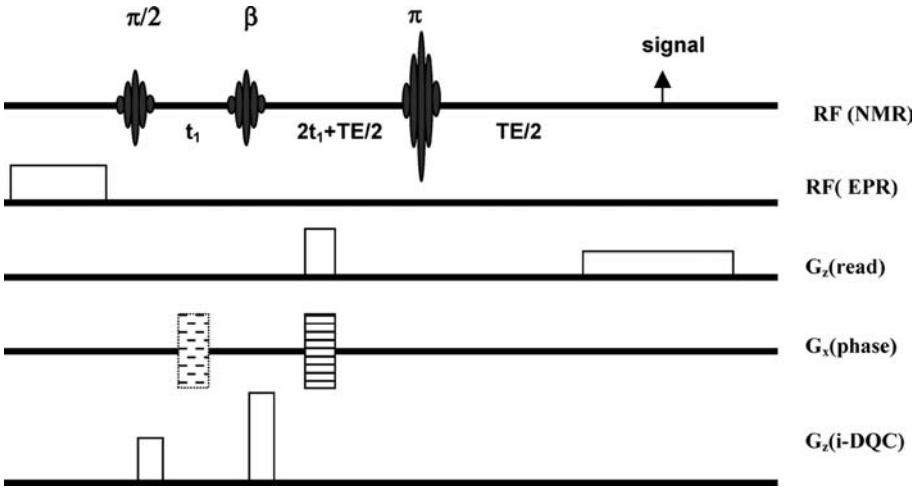

Fig. 1. Pulse sequence used to obtain i-DQC Overhauser images at a magnetic field of 16 mT. Phase encoding gradients G_x (phase) where applied either in the acquisition period or during the DQC evolution interval (dotted rectangle).

during a polarization time interval $T(\mathrm{EPR}) = 500$ ms preceding the CRAZED sequence. A $\pi/2$ pulse at the proton NMR frequency is then applied followed, at time $t_1 = 20$ ms, by another $\beta = \pi/2$ pulse. These two RF pulses, in conjunction with the two i-DQC gradient pulses applied along the z-axis, produce an echo signal at time $2t_1 = 40$ ms after the β pulse. Although the isochromats subsequently dephase, due to magnetic field inhomogeneity, the i-MQC continues to grow and can be refocused by the π pulse applied at time $2t_1 + \mathrm{TE}/2$ after the β pulse. Choosing $\mathrm{TE}/2 = 80$ ms, the total time of i-DQC during the period of acquisition of the single-quantum coherence was $t_2 = 2t_1 + \mathrm{TE} = 200$ ms.

The G_x (phase) channel of Fig. 1 shows a $T_{\mathrm{ph}} = 9$ ms phase encoding gradient pulse. It can be applied during the acquisition period, between the gradient pulse of area 2GT and the π pulse. Moreover, it can also be applied during the i-DQC evolution time, following the G_z i-DQC conversion gradient of area GT, as shown by the dashed rectangles of Fig. 1. In the latter case, the double-quantum evolution reduces the field of view in the phase encoding direction $(\mathrm{FOV})_{\mathrm{phase}}$ by a factor of two compared to phase encoding during the acquisition period [27]. This reduction can be used as a pictorial test for i-DQC imaging.

Coherence gradients of duration $T = 9$ ms and amplitudes $G = 2.4$ and $2G = 4.8$ mT/m were applied along the z-direction. For i-DQC images, reading gradients of duration $T_{\mathrm{r}} = 9$ and $T_{\mathrm{r}} = 18$ ms were also applied along the z-direction with the latter pulse placed at the center of the acquisition window.

Given that the correlation distance [20], determined by half the pitch of the magnetization helix $d = \pi/\gamma\mathrm{GT}$, is approximately 0.55 mm, which is much smaller than the diameter of the cylindrical phantom, overall loss of signal due to correlation with surrounding magnetization [20,28] was not observable for this geometry. Possible interference within the observation window caused by remnants of direct single quantum (SQ) signal was also found to be negligible [28]. As a test of a purely i-MQC effect, the signal amplitude was found to vanish when the double-quantum conversion gradients were applied at the magic angle with respect to the polarizing field.

Fig. 2a shows a normal Overhauser image of the phantom at a magnetic field of 16 mT with in-plane pixel size of 0.43 mm, slice thickness of 20 mm, $N_{\mathrm{S}} = 2$ scans and a 128×128 acquisition matrix. Fig. 2b shows an i-DQC image of the same phantom with the phase encoding gradient applied in the double-quantum conversion interval. The in-plane pixel size was 0.86 mm with slice thickness of 20 mm, 64×64 acquisition matrix and $N_{\mathrm{S}} = 4$ scans. Finally, Fig. 2c shows an image of the phantom with the same values of the phase encoding and read gradients as in Fig. 2b but with the phase encoding gradient applied in the reconversion interval. As expected for a i-DQC image [27], the $(\mathrm{FOV})_{\mathrm{phase}}$ in the phase encoding direction is increased by a factor of two with respect to Fig. 2b, resulting in an elliptical image.

We conclude that Overhauser i-DQC images at very low magnetic field are feasible even under non-ideal conditions. A surprising and somewhat puzzling observation is that the i-DQC signal amplitude is larger, at least by a factor of two, than expected from a straightforward application of Eq. (1) with τ_{d} simply scaled by the Overhauser enhancement. This has also been confirmed by careful measurements of spin–echo signal amplitudes as a function of t_2. In high magnetic fields, diffusion and radiation damping effects [14,17,18] can substantially reduce the i-DQC amplitude from the theoretical value given by Eq. (1). Although these effects should be rather negligible at very low magnetic fields for $t_2 \approx 200$ ms, and therefore a comparatively better performance could be expected, the signal amplitudes

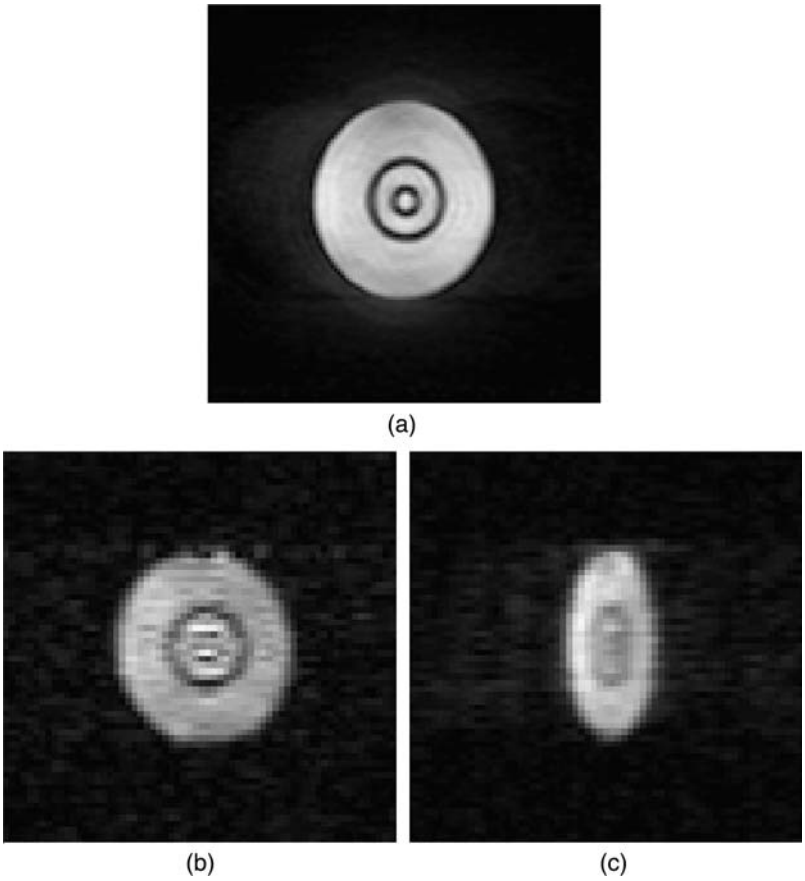

Fig. 2. Overhauser images of a cylindrical phantom at a magnetic field of 16 mT. (a) Normal (SQC) spin–echo image with in-plane pixel size of 0.43 mm, slice thickness of 20 mm, matrix size 128×128, $N_S = 2$ scans, FOV = 55 mm, and spin–echo time = 30 ms. (b) i-DQC image with the phase encoding gradient applied in the DQC evolution period. In plane pixel size 0.86 mm, slice thickness 20 mm, matrix size 64×64, $N_S = 4$ scans, and FOV = 110 mm. (c) i-DQC image obtained under identical conditions as in (b) except that the phase encoding gradient was applied during the acquisition interval. An increase of $(FOV)_{phase}$ by a factor of two with respect to (b) is apparent.

obtained from an analysis of Fig. 2 actually exceed the theoretical value predicted by Eq. (1). This suggests that the process of i-MQC formation under the present conditions may require a more refined analysis.

Acknowledgments

We wish to thank Humberto Vasconcelos Beltrão Neto for able assistance. This work has been supported by Conselho Nacional de Desenvolvimento Científico e Tecnológico (Brazilian agency).

References

[1] S. Vathyam, S. Lee, W.S. Warren, Homogeneous NMR spectra in inhomogeneous fields, Science 262 (1996) 92–96.
[2] R. Bowtell, P. Robyr, Structural investigations with the dipolar demagnetizing field in solution NMR, Phys. Rev. Lett. 76 (1996) 4971–4974.
[3] W. Richter, M. Richter, W.S. Warren, H. Merkle, P. Andersen, G. Adriany, K. Ugurbil, Functional magnetic resonance imaging with intermolecular multiple-quantum coherences, Magn. Reson. Imaging 18 (2000) 489–494.
[4] J. Zhong, Z. Chen, E. Kwok, New image contrast mechanisms in intermolecular double-quantum coherence in human MR imaging, J. Magn. Reson. Imaging 12 (2000) 311–320.
[5] S. Capuani, M. Alesiani, F.M. Alessandri, B. Maraviglia, Characterization of porous media structure by nonlinear NMR methods, Magn. Reson. Imaging 19 (2001) 319–323.
[6] J. Zhong, Z. Chen, E. Kwok, S.D. Kennedy, Enhanced sensitivity to molecular diffusion with intermolecular double-quantum coherences: implications and potential applications, Magn. Reson. Imaging 19 (2001) 33–39.
[7] J. Zhong, E. Kwok, Z. Chen, fMRI of auditory stimulation with intermolecular double-quantum coherences (iDQCs) at 1.5 T, Magn. Reson. Med. 43 (2001) 356–364.
[8] S. Gutteridge, C. Ramanathan, R. Bowtell, Mapping the absolute value of M_0 using dipolar field effects, Magn. Reson. Med. 47 (2002) 871–879.
[9] R. Kimmich, I. Ardelean, Intermolecular multiple-quantum coherence transfer echoes and multiple echoes in nuclear magnetic resonance, J. Chem. Phys. 110 (1999) 3708–3713.
[10] E.D. Minot, P.T. Callaghan, N. Kaplan, Multiple echoes, multiple quantum coherence, and the dipolar field: demonstrating the significance of higher order terms in the equilibrium density matrix, J. Magn. Reson. 140 (1999) 200–205.

[11] J. Jeener, Equivalence between the classical and the "Warren" approaches for the effects of long range dipolar couplings in liquid nuclear magnetic resonance, J. Chem. Phys. 112 (2000) 5091–5094.
[12] W.S. Warren, W. Richter, A.H. Andreotti, B.T. Farmer II, Generation of impossible cross-peaks between bulk water and biomolecules in solution NMR, Science 262 (1993) 2005–2009.
[13] Q. He, W. Richter, S. Vathyam, W.S. Warren, Intermolecular multiple-quantum coherences and cross correlations in solution nuclear magnetic resonance, J. Chem. Phys. 98 (1993) 6779–6800.
[14] S. Lee, W. Richter, S. Vathyam, W.S. Warren, Quantum treatment of the effects of dipole–dipole interactions in liquid nuclear magnetic resonance, J. Chem. Phys. 105 (1996) 874–900.
[15] R. Bowtell, R.M. Bowley, P. Glover, Multiple spin echoes in liquids in a high magnetic field, J. Magn. Reson. 88 (1990) 643–651.
[16] W. Richter, W.S. Warren, Intermolecular multiple quantum coherences in liquids, Concep. Magn. Reson. 12 (2000) 396–409.
[17] W.S. Warren, S. Lee, W. Richter, S. Vathyam, Correcting the classical dipolar demagnetizing field in solution NMR, Chem. Phys. Lett. 247 (1995) 207–214.
[18] C. Ramanathan, R. Bowtell, Dynamics of nuclear magnetic COSY-revamped by asymmetric *z*-gradients (CRAZED) experiment, J. Chem. Phys. 114 (2001) 10854–10859.
[19] P.L. de Sousa, R.E. de Souza, M. Engelsberg, L.A. Colnago, Mobility and free radical concentration effects in proton–electron double-resonance imaging, J. Magn. Reson. 135 (1998) 118–125.
[20] R. Bowtell, S. Gutteridge, C. Ramanathan, Imaging the long-range dipolar field in structured liquid state samples, J. Magn. Reson. 150 (2001) 147–155.
[21] C.H. Tseng, G.P. Wong, V.R. Pomeroy, R.W. Mair, D.P. Hinton, D. Hoffmann, R.E. Stoner, F.W. Hersman, D.G. Cory, R.L. Walsworth, Low-field MRI of laser polarized noble gas, Phys. Rev. Lett. 17 (1998) 3785–3788.
[22] W. Barros Jr., M. Engelsberg, Ionic transport, reaction kinetics, and gel formation. A low-field overhauser magnetic resonance imaging study, J. Phys. Chem. A 106 (2002) 7251–7255.
[23] P.L. de Sousa, M. Engelsberg, M.A. Matos, L.A. Colnago, Measurements of water transport in a gel by Overhauser magnetic resonance imaging, Meas. Sci. Technol. 9 (1998) 1982–1988.
[24] G.C. do Nascimento, R.E. de Souza, M. Engelsberg, A simple, ultralow magnetic field NMR imaging system, J. Phys. E 22 (1989) 774–779.
[25] Nycomed Innovation AB, Malmö, Sweden (proprietary compound).
[26] N. Bloembergen, R.V. Pound, Radiation damping in magnetic resonance experiments, Phys. Rev. 95 (1954) 8–12.
[27] S.S. Velan, P.T. Narasimhan, R.E. Jacobs, MR imaging with phase encoding of intermolecular multiple quantum coherences, J. Magn. Reson. 152 (2001) 189–194.
[28] C. Ramanathan, R. Bowtell, NMR imaging and structure measurements using the long-range dipolar field in liquids, Phys. Rev. E 66 (2001), 041201-1-041201-10.